Review of an Airborne Lightning Detection System and Atmospheric Conditions During Flights in Coastal Thunderstorm Conditions

Zachary Milani[†‡], Leonid Nichman[‡], Edgar Matida[†], Mathieu Lachapelle[‡], Cuong Nguyen[‡], Eric Bruning[§], Mengistu Wolde[‡], Greg M. McFarquhar[‖], Pavlos Kollias[#], R. Timothy Patterson[†]

[†]*Carleton University, Ottawa, Ontario, K1S 5B6, Canada*
[1]ZacharyMilani@cmail.carleton.ca
[3]Edgar.Matida@carleton.ca
[10]Tim.Patterson@carleton.ca

[‡]*National Research Council of Canada, Ottawa, Ontario, K1V 1J8, Canada*
[2]Leonid.Nichman@nrc-cnrc.gc.ca
[4]Mathieu.Lachapelle@nrc-cnrc.gc.ca
[5]Cuong.Nguyen@nrc-cnrc.gc.ca
[7]Mengistu.Wolde@nrc-cnrc.gc.ca

[§]*Texas Tech University, Lubbock, TX 79409-1053, USA*
[6]Eric.Bruning@ttu.edu

[‖]*University of Oklahoma, Norman, OK 73072-7304, USA*
[8]mcfarq@ou.edu

[#]*Stony Brook University, Stony Brook, NY 11794-5000, USA*
[9]pavlos.kollias@stonybrook.edu

Abstract—
Lightning poses a significant risk to aircraft safety, especially as the aviation industry transitions from conventional to hybrid and electric aircraft. It is becoming more common to rely on remotely piloted aircraft systems (RPAS), unmanned aerial vehicles (UAVs), and vertical take-off and landing aircraft (VTOLs) for all-weather aerial activities like transportation and the delivery of goods. Important flight operations decisions of postponing or diverting flights due to severe weather are reliant on accurate information about the presence of lightning and its type, location, flash rate, and information about the ambient conditions inducive of lightning. At present, numerous well-established ground and satellite-based methods exist for monitoring lightning activity. At best, aircraft can receive weather updates from ground sources every 2.5 to 5 minutes, but it is not uncommon for updates to be intermittent due to connection and service stability issues. Therefore, an aircraft-mounted lightning locator may be the most practical source of real-time lightning information for pilots. Detailed performance metrics with uncertainties for commercial airborne lightning locating systems are typically not published and the literature investigating such systems is limited. Here, we present airborne lightning measurements obtained using the commercially available Stormscope Weather Mapping System (WX-500 Series 2; ~1 to 100 kHz). This single-station direction-finding sensor was installed on the Convair-580 research aircraft owned and operated by the National Research Council of Canada (NRC) during the 2022 Experiment of Sea Breeze Convection, Aerosols, Precipitation, and Environment (ESCAPE) campaign in Houston, Texas, which targeted convective updrafts (up to 30 m/s). Stormscope performance is assessed through comparisons to high-quality datasets of total lightning activity provided by the Houston Lightning Mapping Array (HLMA; 60 to 66 MHz) and the GOES - Geostationary Lightning Mapper (GLM; 777 nm). Preliminary results show the Stormscope registered lightning activity in less than 60% of detection windows containing at least one HLMA flash. When considering only single and clustered flashes, Stormscope bearing accuracy was ±12° while the range was often overpredicted and with a large spread. Also presented are in-flight microphysics data including high-resolution images of single particles within in a lightning producing cell.

***Keywords*— Lightning, Flash, Airborne, Microphysics, Cloud**

I. Introduction

Lightning poses a significant risk to aircraft safety, especially as the aviation industry transitions from conventional to hybrid and electric aircraft. Real-time lightning data can be especially important to pilots to safeguard against direct strikes which are estimated to occur on average once per year or every 3000 flight hours [1], and to help avoid regions of strong wind shear, convective updrafts, heavy precipitation, and the abundance of ice hydrometeors that can be associated with lightning. While commercial aircraft are certified to fly in lightning, the number of incidents in which lightning penetrates through aircraft skin are indicative of deficiencies in the

certification process by means of compliance. The abundance of the emerging nonstandard small aircraft for personal air mobility makes the certification even more questionable.

There are many ground-based networks and satellite instruments in operation which continuously monitor lightning activity and can provide near real-time data products to end users like pilots. Through paid subscription services like SiriusXM Aviation, pilots have access to weather and lightning information with an industry leading update rate of (at best) 2.5 minutes, or through free services like ADS-B which has data updates every 5 minutes. These services are extremely valuable for flight planning but when pilots must circumnavigate dangerous conditions in-flight, they are best served by truly real-time data. Paid subscription services also require a stable uplink connection and are only available over select regions (e.g., broad coverage over the CONUS and Southern Canada). Similar to how on-board radar provides pilots with real-time weather information, an aircraft-mounted lightning locator might be the most practical source of real-time lightning information for pilots.

There are three common commercial airborne direction-finding (DF) systems built to map lightning from an aircraft: the 'Stormscope' [2], the LSZ-850/860 [3], and the Insight Strikefinder. To the author's knowledge, the manufacturers of these systems have not published clear performance metrics with uncertainties and the literature on airborne measurements of cloud discharges is limited to declassified government reports from the 70's and 80's. Baum & Seymour [4], [5] compared an early Stormscope model to a very high frequency (VHF) array but their analysis uses data accumulated over minutes (between 4 and 8 mins), does not distinguish between discharge processes types (cloud/cloud-to-ground), nor does it estimate detection efficiency. Walko & Reazer [6] compared the Stormscope to a custom-built airborne DF sensor (which was likely the early version of the LSZ-850) and provides an estimate for Stormscope cloud-to-ground detection efficiency. Given i) the availability of high-quality lightning datasets; ii) the expected increase in the intensity and frequency of extreme weather events along with global temperatures [7]; iii) the aviation industry transitioning from conventional to hybrid, and electric, and hydrogen fueled aircraft; and iv) the projected increase in global flight operations (U.S flight operations are forecast to increase by 24% over the next twenty years [8]), it is important to further investigate the ability of airborne warning systems to detect and avoid severe weather and lightning, and to identify where this technology can benefit from further research and development.

This study presents airborne atmospheric and lightning measurements that were obtained in coastal thunderstorm conditions using a suite of instruments that includes the commercially available Stormscope Weather Mapping System (WX-500 Series 2; ~1 to 100 kHz). Airborne measurements were conducted using the Convair-580 research aircraft owned and operated by the National Research Council of Canada (NRC) during the Experiment of Sea Breeze Convection, Aerosols, Precipitation, and Environment (ESCAPE) [9] campaign in Houston, Texas, which targeted convective updrafts and ran from May to June in 2022. This work compares the airborne lightning data collected to the total lightning activity dataset provided by the Houston Lightning Mapping Array (HLMA; 60 to 66 MHz) and the Geostationary Lightning Mapper (GLM; 777 nm) on the Geostationary Operational Environmental Satellite (GOES). In addition, this work presents the atmospheric data collected during six transects of a lightning producing cell, which includes atmospheric state and the single-particle and bulk microphysical properties of clouds. The microphysical and flash properties of the electrified cell are used to examine its development through time and at five different altitudes.

II. . METHODS

The Stormscope antenna assembly is a flat, low-profile housing mounted to the underside of the Convair-580's fuselage behind the wings. The device consists of a magnetic crossed-loop antenna and a single mono pole antenna to measure the polarity of the electric field. The data processing unit is located inside the cabin. The Stormscope operates in four basic steps: i) signals are filtered by comparing their transient waveform to those of known lightning processes; ii) range distance is determined based on a ratio of the electric and magnetic signal intensities of lightning emission pulses; iii) bearing direction is determined using the magnetic field signal intensities from the crossed-loop antenna; and iv) range distance is corrected / manipulated for individual strikes in an attempt to cluster strikes that are close to one another. The processing unit sends a message block to the multi-function display on the flight deck every 2 s (±0.5 s), which includes all lightning data since the last message block was sent. Each message block sent by the processing unit is also recorded by the aircraft data logger. Each message block is rounded to the nearest second by the data logger during pre-processing.

Flash data from the HLMA and GLM are included in this work. The HLMA is a ground network of more than 12 VHF sensors (60 to 66 MHz) located in and around the Greater Houston Area that maps the 3-D location of total lightning activity in real time using time of arrival (TOA) geolocation [10]. The HLMA detects nearly 90% of flashes within a 300 km radius of its centroid location. The GLM uses a charged-coupled device sensor to measure the line-of-sight intensity of the electromagnetic emissions from total lightning activity at a wavelength of 777 nm (385833 GHz) [11].

The Stormscope is one of the many probes and sensors integrated onboard the NRC Convair-580 airborne research laboratory, which is a heavily modified twin engine turbo-prop aircraft capable of performing airborne atmospheric measurements [12], [13], [14], [15]. The temperature, pressure, and updraft velocity are sampled at 1 Hz resolution. The liquid water content (LWC) measurements are collected at 1 Hz resolution using the Nevzorov hot-wire probe [16]. Several imaging probes are used to investigate the many different hydrometeor sizes present in a thunderstorm environment. The 2-D stereo probe (2D-S, SPEC Inc.) [17] and high-volume precipitation spectrometer Ver. 3 (HVPS-3, SPEC Inc.) are used to continuously image hydrometeors over a large size

range, spanning several orders of magnitude from ~10 to 19,200 µm in diameter [18]. High-resolution hydrometeor images are captures by the Cloud Particle Imager (CPI, 15 – 2,500 µm, SPEC Inc.) and classified using an in-house convolutional neural network classification algorithm similar to [19].

III. Results and Discussion

A. Stormscope Detection Efficiency

To temporally compare lightning activity between datasets, the mean flash times from the HLMA [20] were discretized into 2 s bins equal to the Stormscope, and the data within each bin are reported at the time defined by the right bin edge. The Stormscope measured lightning activity in 54% of detection windows that contained at least one HLMA flash during ESCAPE Flight 4 (henceforth referred to as CRF04), of which there were 5423 total windows. Using a rudimentary cloud / cloud to ground filter, it is estimated that less than 3 % of detection windows with at least one HLMA flash presented evidence of a cloud to ground strike making one this of the largest detection efficiency analyses of cloud flashes found in the literature for an airborne lightning sensor.

The DF design of the Stormscope makes it ideal for measuring cloud to ground return strokes and although it's not necessarily designed for it, the Stormscope can also measure strong cloud discharges [21]. It's possible the non-vertical and meandering nature of cloud lightning channels produces slightly altered waveforms that are not recognized or properly processed by the Stormscope, which may account for the reduced detection efficiency when compared to the HLMA. During CRF04, there were 73 detection windows (of 2975 in total) containing Stormscope activity and no HLMA activity which suggests a reasonably low false positive detection rate of ~2.5 %.

The important takeaway is the Stormscope missed more than 40% of detection windows containing cloud activity. Given that cloud flashes are much more common than CG flashes and pose a direct threat to aircraft safety, this finding identifies an aspect of the modern airborne lightning locating system that could be improved. A more comprehensive assessment of Stormscope performance during the ESCAPE campaign will be provided in the presentation that accompanies this paper.

B. Bearing and Range Estimation

This work uses an analytical solution to predict the site errors for a DF sensor equipped to an aircraft [22] rather than specialized ground equipment like a pulse generator. HLMA flash data from CRF04 were filtered to identify single and clustered flashes for this bearing accuracy analysis. Stormscope bearing error is defined as the angular difference between the mean HLMA and Stormscope bearings. The Stormscope bearing error for CRF04 has a σ of ±12° which agrees with the average bearing error of ±11° found in the literature [4], [5]. The bearing error distribution shows a slight bias towards positive values due to the theoretical nature of the analytical error model not accounting for factors that affect the real measurements. This slight bias does not affect the interpretation of results. Rather, the agreement between the bearing errors in this work and the literature proves that this practically simple, analytical model can be used as an error estimation tool in the absence of specialized calibration equipment.

Minimum range is used to analyse the Stormscope distance accuracy because if several flashes are detected, knowledge about the minimum distance to lightning activity is important to avoid travelling near dangerous clouds or regions with a high electric field. The scatter plot in Figure 1 compares the minimum distance to lightning activity as measured by the HLMA and Stormscope for 2 s detection windows that contained single and clustered flashes. Figure 1 shows how the Stormscope overpredicted minimum flash distance in ~84 % measurements during CRF04. The average range error is ~40 nmi which is larger than the ±20 nmi error that is reported throughout the literature [4], [5], [6], [23]. Due to the techniques the Stormscope uses to calculate range, it is possible for strong distant flashes to resemble weak nearby flashes and vice-versa. Although elevated range errors are generally expected when using this type of system, it could be possible to improve the range estimates by applying modern signal processing techniques like those described in Refs. [24], [25], [26], [27].

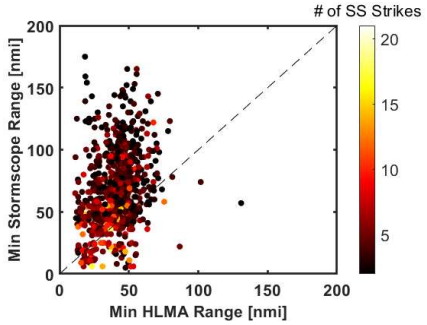

Figure 1: Comparing the Stormscope and HLMA measurements for minimum distance to lightning activity during CRF04. The heatmap shows the number of Stormscope strikes within each 2 s detection window.

C. Transects Through Lightning Producing Cell

During ESCAPE Flight 12 (henceforth referred to as CRF12) which took place from 20:46 UTC on June 16th to 00:41 UTC on June 17th, 2022, the aircraft collected data along the western boundaries of a multi-cell storm with widespread lightning production. At around 23:10 UTC the aircraft began transecting a developing cell which had a reflectivity core > 45 dBZ but had not yet produced lightning. The aircraft transected the cell six times at five different altitudes while collecting environmental data that included static temperature, pressure, updraft velocity, water content, images of cloud hydrometeors, and Stormscope lightning locations.

Figure 2 is an 8-tile plot presenting the Next Generation Weather Radar (NEXRAD) 4bit base reflectivity mosaic offered by the Iowa Environmental Mesonet Web Mapping Service at 5-minute intervals [28], the aircraft flight path as it sampled the cell, and the flash locations from all available sensors and networks.

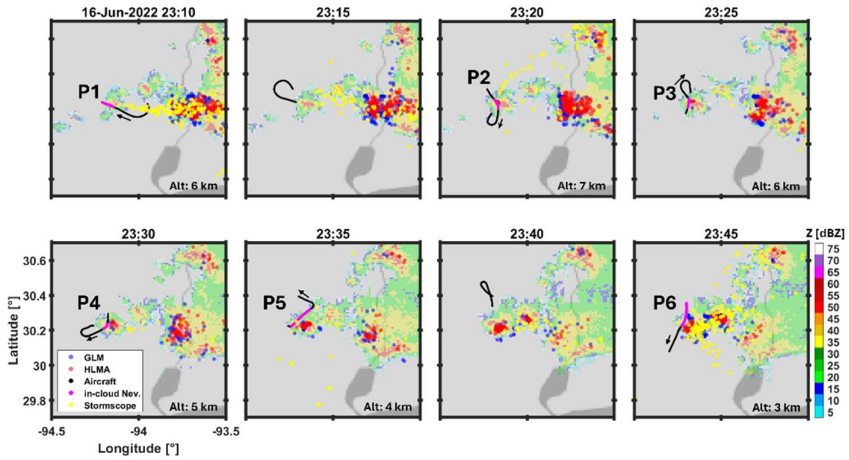

Figure 2: An 8-tile plot showing NEXRAD mosaic of base reflectivity, the aircraft flight path as it sampled the cell, and flash locations at 5-minute intervals during CRF12 on June 16th, 2022.

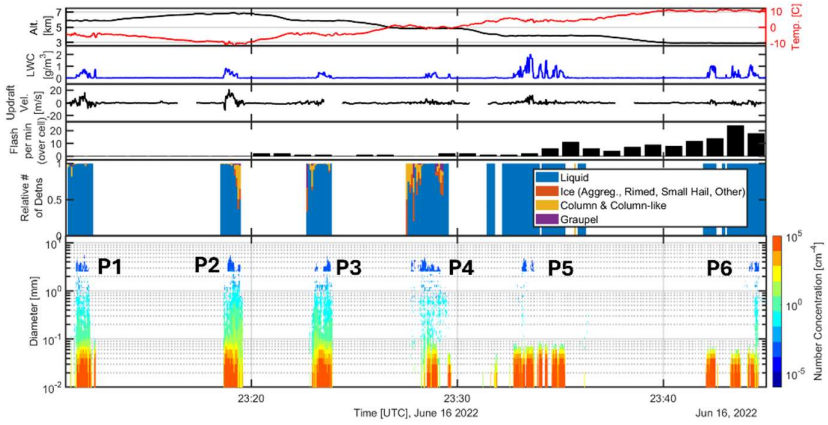

Figure 3: Time series plot for temperature, altitude, water content (liquid and total), flash rate, habit classification, and composite particle size distribution for Passes 1 through 6 during CRF12 on June 16, 2022.

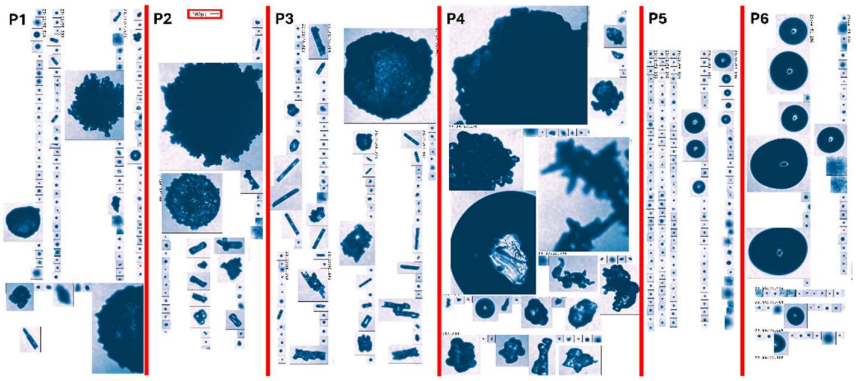

Figure 4: Single-particle hydrometer images collected by CPI for Passes 1 through 6 during CRF12 on June 16, 2022.

Each NEXRAD mosaic corresponds to the indicated time above each tile, while the aircraft flight path and lightning data span an interval ±2.5 minutes of indicated time.

Figure 2 shows no overhead flashes were detected during Pass 1. The HLMA first detected activity over the sampled cell during Pass 3 and this low activity level persists during the next pass. By Pass 5 the aircraft had to avoid travelling directly through reflectivity core due to the dangerous conditions within the developing cell inferred from the increased number of flashes overhead. Shortly after Pass 5, the large cell to the east, which had been producing most of the lightning flashes in the immediate area, was beginning to weaken and its lightning production declining. At 20:40 UTC, the cell positioned in-between the sampled cell and the cell to the east started to produce flashes. By the time Pass 6 was performed, the flash rate overtop of the sampled cell had increased significantly. Nearly all flashes generated by the sampled cell had a mean altitude greater than 8 km as measured by the HLMA. By the time Pass 6 was complete, the cell had a max flash rate of 24 flashes/min and this trend was increasing (see Figure 3).

Passes 2, 3, 4, and 6 have sections that are nearly co-located along the North-South heading. These passes were performed at altitudes of roughly 7, 6, 5, and 3 kms, respectively and data from these passes can be used to infer the vertical structure of the lightning-producing cell. Figure 3 shows the time series data for passes 1 through 6 which includes static temperature, pressure, water content (liquid and total) [29], updraft velocity [30], flash rate per minute, hydrometeor habit classification, and the composite particle size distribution, which derived the dimensions of hydrometers using the minimum enclosing circle technique [31]. The updraft velocity data presented in the third panel of Figure 3 has intervals in which data are missing; this is intentional, and the result of a quality control procedure meant to remove periods of poor data quality. Data quality could be affected by, e.g., temporary ice accretion on the probe. Figure 4 presents high-resolution single-particle images collected by the CPI for each pass.

At 7 km and -10 °C, Pass 2 recorded LWC values near 1 g/m^3 and the highest updraft velocity of all passes near 20 m/s. The habit classification plot shows how the proportion of ice hydrometeors was relatively large near the end of the transect or the south-side of cell when compared to the northwest-side. The highest concentration of particles in the size distribution are hydrometeors < 100 µm in diameter, dominated by liquid droplets. Hydrometers with moderate to large sizes (100µm < diameter < 1 mm) are present in lower concentrations and are observed in Figure 4 to be mostly graupel or hail, columns (or other hydrometers with a sizable aspect ratio), and some rimed ice particles. The largest hydrometeors (> 1 mm) are observed in Figure 4 to be graupel or hail particles. These large hydrometers exist in relatively low number concentrations but hold a significant proportion of the total water content. This diverse population of hydrometeors with different phases and sizes coupled with large updraft velocities promotes the charge transferring collisions and the subsequent separation (advection) of the newly charged particles which is a precursor for cloud electrification. The first lightning flashes produced by this cell were measured by the HLMA as the aircraft exited the cell.

At 6 km and -4 °C, Pass 3 is a near mirror image of Pass 2 since the aircraft flew in the opposite South to Northwest direction while closely following the previous flight path. The hydrometer population at the south-side of the cell was still more strongly mixed when compared to the northwest-side. Notably, more pristine columns and aggregate columns are observed at this altitude which has a slightly higher temperature. Large graupel hydrometeors are also still observed, and the flash rate was at steady but low levels during Pass 3 (< 5 flashes/min).

At 5 km and roughly 0 °C, Pass 4 entered the cell from the north direction rather than travelling through the northwest side of the cell like the previous passes. A relatively large fraction of the hydrometeor population leading up to and following the penetration of the cell's core was classified as ice habits (more than in previous passes). The large fraction of ice hydrometeors outside the cell is evident of the strong updraft rising through the cell's core which pushes the falling ice particles towards the cell edges. The total number concentration of moderate to large sized hydrometeors (100µm < diameter < 1 mm) within the core is reduced when compared to previous passes. The particle images in Figure 4 show a variety habits including large graupel and hail, frozen drops, dendritic particles, large raindrops, and other riming ice particles. The cell's flash rate was unsteady throughout Pass 4 and reached the level of < 5 flashes/min upon completion of the transect.

At 3 km and 8 °C, Pass 6 measured relatively low updraft velocities and high LWC levels due to the melting of solid hydrometeors into the liquid phase as they fall and spend time above freezing temperatures. These elevated LWC levels were also observed during Pass 5. The hydrometeor populations for these passes are nearly all liquid water, which is confirmed by the habit classification results and the particle images which show a mixture of large and small droplets. The particle size distribution shows practically none of the moderately sized solid hydrometers at this altitude. Large raindrops are observed likely due to the coalescence combination of smaller droplets as they fall and collide. The flash rate level is relatively high during Pass 6 and follows an increasing trend.

In addition to the four co-located passes, two passes (P1 and P3) were performed at the same 6 km altitude. Passes 1 and 3 were separated temporally by ~15 minutes and occurred before and after the first flashes were produced by the cell. The habit classification in Figure 3 shows how larger fractions of ice particles are observed during Pass 3, however, this could be caused by the aircraft sampling different parts of the cloud. The particle images in Figure 4 show how the columns observed during Pass 3 appear to have a larger aspect ratio and some columns are aggregated or been subject to riming. So far, there has been no observation of chain aggregates of ice crystals or other habits that can be formed by the electric field alignment of ice crystals [32], but work to identify these types of particles is ongoing.

Future work with these data includes attempting to calculate the surface area, mass, and shape factor of the different liquid

and solid phase hydrometeors which, when coupled with updraft velocity, may be used to estimate mass flux of components within the cell. With mass flux estimates, the hypothesis that total lightning frequency is roughly proportional to the downward mass flux of solid hydrometers (graupel) and upward mass flux of ice crystals can be further tested [33]. In-situ data like those presented in the study can also be used to validate radar products that attempt to characterise the microphysical properties of lightning producing clouds.

Future airborne measurements of lightning-producing clouds would benefit from higher altitude sampling (near flash altitude), and the direct measurement of single particle charge and mass. These technologies are not yet available but would significantly improve our understanding of how exactly clouds become electrified. Furthermore, flying a radar pass prior to the planned transect would allow for validation of the airborne radar products indicative of electrification, using in-situ microphysics data.

CONCLUSIONS

Along with a suite of other atmospheric sensing instruments, the Stormscope Weather Mapping System (WX-500 Series 2; ~1 to 100 kHz) was installed on the NRC Conviar-580 research aircraft during the 2022 ESCAPE campaign in Houston, Texas, which targeted strong convective updrafts. This study reviews data collected throughout two flights lasting about four hours each: CRF04 on June 4th and CRF12 on June 16-17th, 2022.

The Stormscope site errors were corrected using an analytical solution rather than ground equipment. CRF04 lightning data were carefully filtered according to which Stormscope performance metric was assessed. Key performance findings include: i) the Stormscope measured lightning activity in 54% of detection windows with at least one HLMA flash; and ii) the Stormscope bearing accuracy was ±12 deg which is withing good agreement of literature values; and iii) the Stormscope tends overpredicts the range to lightning.

During CRF12, the aircraft transected a lightning producing cell six times at five different altitudes while equipped with a suite of environmental probes and sensors. The aircraft measured upwards of 25 m/s updraft velocities within the core of the cell. Several different solid hydrometeor habits were imaged outside of the core, as they were falling, at all altitudes above the freezing layer. The images include large graupel and hail, columns (aggregate and pristine), dendrites, moderately sized ice particles and liquid droplets spanning small to large sizes.

Future work includes using these in-situ data to further test the hypothesis that total lightning frequency is roughly proportional to the mass flux of solid hydrometers within the cloud.

ACKNOWLEDGMENT

The authors acknowledge the co-PIs of the ESCAPE campaign, weather forecasters, flight crew, and instrumentation and maintenance teams that made the ESCAPE campaign successful. We thank the National Science Foundation for major support of ESCAPE. The authors would like to acknowledge the following NSF grants: AGS-2019932, AGS-2019968, AGS-2019939. The authors would also like to acknowledge the National Research Council of Canada (NRC) Aeronautical Product Development and Certification (APDC) program for funding this analysis

REFERENCES

[1] A. Larsson, "The Interaction Between a Lightning Flash and an Aircraft In Flight," *C R Phys*, vol. 3, no. 10, pp. 1423–1444, Oct. 2002, doi: 10.1016/S1631-0705(02)01410-X.

[2] P. A. Ryan and N. Spitzer, "Stormscope," US Patent 4,023,408, 1977.

[3] E. W. Coleman, "LSZ-850 lightning sensor system," in *NOAA International Aerospace and Ground Conference on Lightning and Static Electricity*, 1988, pp. 434–438.

[4] R. K. Baum and T. J. Seymour, "In-Flight Evaluation of a Severe Weather Avoidance System for Aircraft (AFWAL-TR-80-3022)," Flight Dynamics Laboratory (AFWAL), Wright-Patterson AFB, Ohio, May 1980.

[5] T. J. Seymour and R. K., Baum, "Evaluation of the Ryan Stormscope as a Severe Weather Avoidance System For Aircraft Preliminary Report (Rep. FAA-RD-79-6)," in *FAA/FIT Workshop on Grounding and Lightning Technology*, Melbourne, FL, 1979, pp. 29–35.

[6] L. C. Walko and M. J. Reazer, "Data Acquisition for Evaluation of an Airborne Lightning Detection System (AFWAL-TR-83-3083)," Flight Dynamics Laboratory (AFWAL), Wright-Patterson AFB, Ohio, Sep. 1983.

[7] Intergovernmental Panel on Climate Change, "Weather and Climate Extreme Events in a Changing Climate," in *Climate Change 2021 – The Physical Science Basis*, Cambridge University Press, 2023, pp. 1513–1766. doi: 10.1017/9781009157896.013.

[8] FAA, "FAA Aerospace Forecast Fical Years 2023 - 2043," 2023.

[9] P. Kollias *et al.*, "Experiment of Sea Breeze Convection, Aerosols, Precipitation and Environment (ESCAPE)," *Bull Am Meteorol Soc*, May 2024, doi: 10.1175/BAMS-D-23-0014.1.

[10] T. Logan, "An Analysis of the Performance of the Houston Lightning Mapping Array During an Intense Period of Convection During Tropical Storm Harvey," *Journal of Geophysical Research: Atmospheres*, vol. 126, no. 3, Feb. 2021, doi: 10.1029/2020JD033270.

[11] S. J. Goodman *et al.*, "The GOES-R Geostationary Lightning Mapper (GLM)," *Atmos Res*, vol. 125–126, pp. 34–49, May 2013, doi: 10.1016/j.atmosres.2013.01.006.

[12] J. R. Minder *et al.*, "P-Type Processes and Predictability: The Winter Precipitation Type Research Multiscale Experiment (WINTRE-MIX)," *Bull Am Meteorol Soc*, vol. 104, no. 8, pp. E1469–E1492, 2023, doi: 10.1175/BAMS-D-22-0095.1.

[13] M. He *et al.*, "Total Organic Carbon Measurements Reveal Major Gaps in Petrochemical Emissions Reporting," *Science (1979)*, vol. 383, no. 6681, pp. 426–432, Jan. 2024, doi: 10.1126/science.adj6233.

[14] E. R. Williams, M. F. Donovan, D. J. Smalley, J. M. Kurdzo, and B. J. Bennett, "The 2017 Buffalo Area Icing and Radar Study (BAIRS II)," 2020.

[15] B. Bernstein *et al.*, "The In-Cloud Icing and Large-Drop Experiment (ICICLE) Science and Operations Plans," 2021.

[16] A. V. Korolev, J. W. Strapp, G. A. Isaac, and A. N. Nevzorov, "The Nevzorov Airborne Hot-Wire LWC–TWC Probe: Principle of Operation and Performance Characteristics," *J Atmos Ocean Technol*, vol. 15, no. 6, pp. 1495–1510, Dec. 1998, doi: 10.1175/1520-0426(1998)015<1495:TNAHWL>2.0.CO;2.

[17] R. P. Lawson *et al.*, "The 2D-S (Stereo) Probe: Design and Preliminary Tests of a New Airborne, High-Speed, High-Resolution Particle Imaging Probe," *J Atmos Ocean Technol*, vol. 23, no. 11, pp. 1462–1477, Nov. 2006, doi: 10.1175/JTECH1927.1.

[18] SPEC Inc, "HVPS V3 Technical Manual: A High Volume Precipitation Spectrometer (Rev 1.2)," Boulder, CO, 2013. [Online]. Available: www.specinc.com

[19] C. Praz, S. Ding, G. M. McFarquhar, and A. Berne, “A Versatile Method for Ice Particle Habit Classification Using Airborne Imaging Probe Data,” *Journal of Geophysical Research: Atmospheres*, vol. 123, no. 23, pp. 13,472-13,495, Dec. 2018, doi: 10.1029/2018JD029163.

[20] Timothy Logan, Eric Bruning, Kelcy Brunner, and Jessica Souza, “Houston Lightning Mapping Array (HLMA) Flash-level data,” UCAR/NCAR - Earth Observing Laboratory. Accessed: Jun. 26, 2024. [Online]. Available: https://doi.org/10.26023/GBKS-E7VT-HS11

[21] A. Nag, M. J. Murphy, W. Schulz, and K. L. Cummins, “Lightning Locating Systems: Insights on Characteristics and Validation Techniques,” *Earth and Space Science*, vol. 2, no. 4, pp. 65–93, Apr. 2015, doi: 10.1002/2014EA000051.

[22] L. Parker and H. Kasemir, “Airborne Warning Systems for Natural and Aircraft-Initiated Lightning,” *IEEE Trans Electromagn Compat*, vol. EMC-24, no. 2, pp. 137–158, May 1982, doi: 10.1109/TEMC.1982.304009.

[23] N. Rasch, W. Lewis, and A. Barile, “Ground Evaluation of an Airborne Lightning Locator System,” Atlantic City, Jun. 1983.

[24] V. Ramachandran, J. N. Prakash, A. Deo, and S. Kumar, “Lightning Stroke Distance Estimation From Single Station Observation and Validation With WWLLN Data,” *Ann Geophys*, vol. 25, no. 7, pp. 1509–1517, Jul. 2007, doi: 10.5194/angeo-25-1509-2007.

[25] Z. Koochak and A. Fraser-Smith, “Single-Station Lightning Location Using Azimuth and Time of Arrival of Sferics,” *Radio Sci*, vol. 55, no. 2, Feb. 2020, doi: 10.1029/2018RS006627.

[26] T. Ogawa and M. Komatsu, “Analysis of Q burst waveforms,” *Radio Sci*, vol. 42, no. 2, Apr. 2007, doi: 10.1029/2006RS003493.

[27] C. Mackay and A. C. Fraser-Smith, “Lightning location using the slow tails of sferics,” *Radio Sci*, vol. 45, no. 5, p. n/a-n/a, Oct. 2010, doi: 10.1029/2010RS004405.

[28] Iowa State University, “Iowa Environmental Mesonet.” Accessed: Jun. 25, 2024. [Online]. Available: https://mesonet.agron.iastate.edu/docs/nexrad_mosaic/

[29] Natalia Bliankinshtein, “ESCAPE: Bulk Properties Data (Version 1.0),” UCAR/NCAR - Earth Observing Laboratory. Accessed: Jun. 26, 2024. [Online]. Available: https://data.eol.ucar.edu/dataset/619.013

[30] Kenny Bala, “ESCAPE: Atmospheric and Aircraft State Data (Version 1.0),” UCAR/NCAR - Earth Observing Laboratory. Accessed: Jun. 26, 2024. [Online]. Available: https://doi.org/10.26023/DW2F-R2DK-WQ00

[31] Greg M. McFarquhar, Mengistu Wolde, Leonid Nichman, Kenny Bala, and Saurabh Patil, “ESCAPE: Optical Array Probes (OAP) Microphysics Data (Version 1.0),” UCAR/NCAR - Earth Observing Laboratory.

[32] P. J. Connolly *et al.*, “Aircraft Observations of the Influence of Electric Fields on the Aggregation of Ice Crystals,” *Quarterly Journal of the Royal Meteorological Society*, vol. 131, no. 608, pp. 1695–1712, Apr. 2005, doi: 10.1256/qj.03.217.

[33] W. Deierling, W. A. Petersen, J. Latham, S. Ellis, and H. J. Christian, “The Relationship Between Lightning Activity and Ice Fluxes in Thunderstorms,” *Journal of Geophysical Research Atmospheres*, vol. 113, no. 15, 2008, doi: 10.1029/2007JD009700.